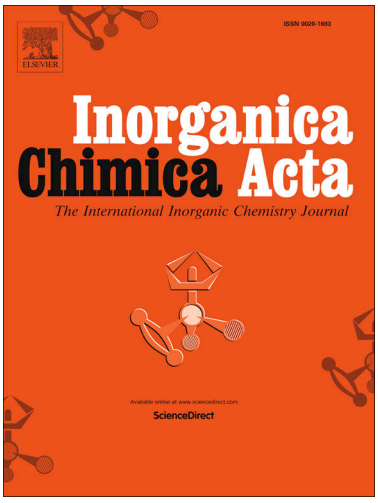
Journal Pre-proofs



A cationic Co(II) coordination polymer $^{1}{}_{\infty}[Co(\mu\text{-}L)(\mu\text{-}Cl)(H_2O)_2]^+$ with the 4-amino-4*H*-1,2,4-triazole ligand: structure, thermal behavior, and antimicrobial activity

Sabri Hassen, Youssef Arfaoui, Yaroslav Filinchuk, Axel Klein, Hammouda Chebbi

PII: S0020-1693(23)00289-X
DOI: https://doi.org/10.1016/j.ica.2023.121664
Reference: ICA 121664

To appear in: *Inorganica Chimica Acta*

Received Date: 13 March 2023
Revised Date: 19 June 2023
Accepted Date: 24 June 2023

Please cite this article as: S. Hassen, Y. Arfaoui, Y. Filinchuk, A. Klein, H. Chebbi, A cationic Co(II) coordination polymer $^{1}{}_{\infty}[Co(\mu\text{-}L)(\mu\text{-}Cl)(H_2O)_2]^+$ with the 4-amino-4*H*-1,2,4-triazole ligand: structure, thermal behavior, and antimicrobial activity, *Inorganica Chimica Acta* (2023), doi: https://doi.org/10.1016/j.ica.2023.121664

This is a PDF file of an article that has undergone enhancements after acceptance, such as the addition of a cover page and metadata, and formatting for readability, but it is not yet the definitive version of record. This version will undergo additional copyediting, typesetting and review before it is published in its final form, but we are providing this version to give early visibility of the article. Please note that, during the production process, errors may be discovered which could affect the content, and all legal disclaimers that apply to the journal pertain.

© 2023 Published by Elsevier B.V.

A cationic Co(II) coordination polymer $^{1}_{\infty}[Co(\mu\text{-}L)(\mu\text{-}Cl)(H_2O)_2]^+$ with the 4-amino-4*H*-1,2,4-triazole ligand: structure, thermal behavior, and antimicrobial activity

Sabri Hassen [a], Youssef Arfaoui [a,*], Yaroslav Filinchuk [b], Axel Klein [c,*],

and Hammouda Chebbi [d,e,*]

[a] *University of Tunis El Manar, Faculty of Sciences of Tunis, Laboratory of Characterizations, Applications and Modeling of Materials, 2092 El Manar II, Tunis, Tunisia. Email: sabrihassen10@gmail.com, ORCID: 0000-0002-9432-8204 (SH); Email: youssef.arfaoui@fst.utm.tn, ORCID: 0000-0003-1615-9502 (YA).*

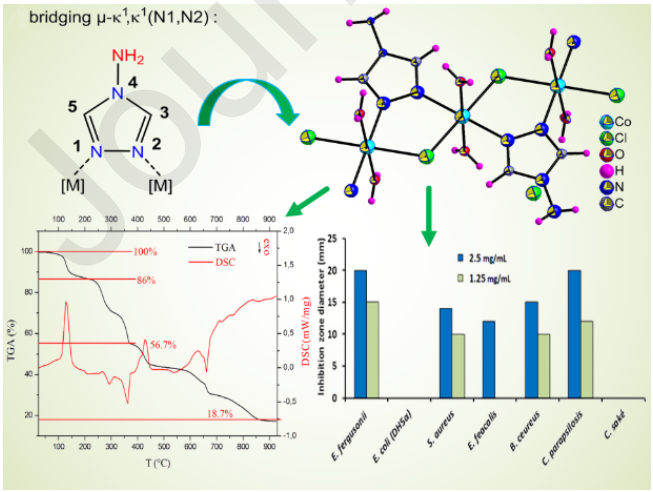
[b] *Institute of Condensed Matter and Nanosciences, Université catholique de Louvain, Place L. Pasteur 1, 1348 Louvain-la-Neuve, Belgium. Email: yaroslav.filinchuk@uclouvain.be, ORCID: 0000-0002-6146-3696 (YF).*

[c] *University of Cologne, Faculty of Mathematics and Natural Sciences, Department of Chemistry, Institute for Inorganic Chemistry, Greinstrasse 6, 50939 Cologne, Germany.*

[d] *University of Tunis, Preparatory Institute for Engineering Studies of Tunis, Jawaharlal Nehru Street, 1089 Montfleury, Tunis, Tunisia.*

[e] *University of Tunis El Manar, Faculty of Sciences of Tunis, Laboratory of Materials, Crystal Chemistry and Applied Thermodynamics, 2092 El Manar II, Tunis, Tunisia.*

Corresponding authors: Hammouda Chebbi, *E-mail: chebhamouda@yahoo.fr;* ORCID: 0000-0002-0726-7053 (HC) Youssef Arfaoui, *Email: youssef.arfaoui@fst.utm.tn*, ORCID: 0000-0003-1615-9502 (YA), and Axel Klein, *Email: axel.klein@uni-koeln.de*, ORCID: 0000-0003-0093-9619 (AK).



Abstract:

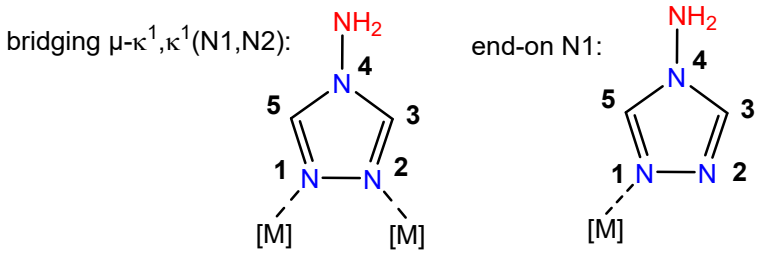
We report a combined experimental and theoretical study on a Co(II) coordination polymer $^{1}_{\infty}$[Co(μ-L)(μ-Cl)(H_2O)$_2$]Cl based on 4-amino-4*H*-1,2,4-triazole (L). Single crystal X-ray diffraction showed that the Co(II) ions are coordinated by the N1 and N2 atoms of the bridging 4-amino-1,2,4-triazole ligand, two *trans*-oriented bridging Cl^- ligands and two O atoms from coordinated water molecules in a distorted octahedral geometry. The ligand shows a bridging μ-κ^1, κ^1,(N,N) coordination with Cl–Cl–N–N–Co five membered rings in the polymeric strand. Intra and intermolecular N–H···O and O–H···Cl hydrogen bonding interactions stabilize the crystal structure. Hirshfeld surface analysis in combination with ATR–FTIR, and FT-Raman spectroscopy were carried out to study the multitude of non-covalent interactions. Geometry optimization using density functional theory (DFT) calculations on the monomolecular model [Co(L)$_2$Cl$_2$(H_2O)$_2$] on B3LYP/6-311++G(2d,2p) level gave good agreement with the metrics found in the crystal structure and also agreed quite well with the experimental IR and Raman data, thus allowing spectral assignments. Thermogravimetric (TGA) and Differential Scanning Calorimetric (DSC) experiments coupled with mass spectrometry (MS) under an argon atmosphere in the temperature range 25 to 950 °C showed thermal stability till about 100 °C. The compound showed inhibitory activity against the Gram-negative bacterium *E. fergusonii*, the Gram-positive bacteria *S. aureus*, *E. feacalis*, and *B. cereus*, and the yeast *C. parapsilosis* in agar diffusion experiments at a concentration of 1.25 and 2.50 mg/mL with inhibition zones of 10 to 20 mm in 24 h, but not against the Gram-negative *E. coli* and the yeast *C. saké*.

Keywords: Co(II) coordination polymer; 4-amino-1,2,4-triazole; crystal structure; thermal properties; DFT; antimicrobial activity.

1. Introduction

Coordination polymers represent a very attractive group of functional materials due their modular synthesis from metal salts and ligands, and their interesting optical, electronic, magnetic, catalytic and biological/pharmacological properties [1–10]. The choice of the metal ion, a well understanding of the coordination preferences of the bridging ligands which are frequently polyfunctional or at least ditopic, and a careful selection of the terminal ligands are key steps for the rational design of coordination polymers with specific structural topologies, as well as chemical and physical properties [1,2,6–10].

The polyfunctional molecule 4-amino-1,2,4-triazole, abbreviated as atrz (or sometimes as NH_2-trz), is a very suitable ligand due to its various coordination modes [11–13] and a large number of coordination polymers with metal such as Mo(IV) [14], Mn(II) [15], Fe(II) [16–20], Fe(III) [18,21], Co(II) [20–24], Ni(II) [20,22], Cu(II) [21,25–31], Cu(I) [32,33], Zn(II) [34,35], Cd(II) [20,28,35,36], and Ag(I) [37,38] have been reported in which atrz bridges two metals using the μ-κ^1,κ^1(N1,N2) coordination (Scheme 1).



Scheme 1. 4-amino-4*H*-1,2,4-triazole (atrz) with numbering and reported coordination modes.

The big number of publications on Fe(II)- and Cu(II)-atrz coordination polymers with interesting magnetic properties [16–21,25–31] stand in contrast to markedly fewer reports on Co(II)-atrz coordination polymers [20–24]. This number gets larger if atrz derivatives with "supporting" ligand functions like pyridines were added to the list [39,40]. Also oligonuclear Co(II)-atrz complexes are scarce [41–46]. End-on N1-binding (Scheme 1) of Co(II) was reported in the coordination polymer $[Co(\mu\text{-ox})(atrz)_2]$ (ox = μ^2,κ^2,κ^2-oxalate) [47], and while the mononuclear $[Co(atrz)_3](NO_3)_2{\cdot}nH_2O$ is registered but was only poorly characterized [48]. Metal–NH_2 coordination of 4-amino-1,2,4-triazole has not been reported yet.

At the same time, various biological activities were reported from 4-amino-4*H*-1,2,4-triazole or close derivatives such as anticancer, anticonvulsant, antioxidant, antifungal, anti-tubercular, anti-inflammatory, antineoplastic, anti-tuberculosis, antimicrobial and tyrosinase inhibition [49–56].

The present study reports the synthesis of a new Co(II) coordination polymer $^1{}_\infty[Co(\mu\text{-L})(\mu\text{-Cl})(H_2O)_2]Cl$ synthesized from $CoCl_2{\cdot}6H_2O$ and 4-amino-4*H*-1,2,4-triazole (atrz) with atrz acting as $\mu\text{-}\kappa^1,\kappa^1$(N1,N2)-bridging ligand. We studied the compound by single crystal X-ray diffraction including Hirshfeld surface analysis, IR, Raman spectroscopy and thermal analysis (TGA/DSC) coupled with mass spectrometry. Density functional theory (DFT) calculations on the molecular entity using the monomolecular model $[Co(L)_2Cl_2(H_2O)_2]$ were used to assign vibrational bands and to investigate the nucleophilic and electrophilic reactive sites. The antimicrobial activity of the title compound against the Gram-negative bacteria *E. fergusonii*, and *E. coli*, the Gram-positive bacteria *S. aureus*, *E. feacalis*, and *B. cereus*, and the yeasts *C. parapsilosis* and *C. saké* was evaluated using the agar diffusion method.

2. Experimental

2.1 Materials and Instrumentation

Solvents and reagents were obtained from commercial sources and used as received $CoCl_2{\cdot}6H_2O$ and 4-amino-4*H*-1,2,4-triazole were obtained from Aldrich. ATR-IR and Raman scattering spectra were recorded on a Bruker Alpha spectrometer equipped with a platinum ATR module (diamond crystal) in the range from 400 to 4000 cm^{-1} and a Bruker FT Raman RFS 100/S spectrometer in the range from 0 to 4000 cm^{-1}, using a 1064 nm laser. Thermogravimetric (TGA) and differential scanning calorimetry (DSC) measurements were carried out under argon atmosphere from 25 to 950 °C using a

Netzsch STA 449 F3 Jupiter TGA/DSC device equipped with a stainless steel oven housed in an argon-filled glovebox and coupled to a Netzsch QMS 403 D Aëolos mass spectrometer. The measurements were performed under an argon flow of 100 mL·min^{-1} at a heating rate of 5 K·min^{-1}. Elemental analyses (C, H, and N) were performed using a Hekatech CHNS EuroEA 3000 Analyzer.

2.2 Synthesis

A solution of 168 mg (2 mmol) 4-amino-4*H*-1,2,4-triazole in 10 mL of EtOH was added dropwise to an aqueous solution (20 mL) of 476 mg $CoCl_2{\cdot}6H_2O$ (2 mmol). The reaction mixture was stirred for 2 h and then left to slow evaporate at room temperature. After 2 weeks, pink block crystals were obtained from a pink solution, supporting that the Co(II) oxidation state is retained after this time. Yield: 418.24 mg (1.68 mmol, 84%). Anal. Calc. for $C_2H_8ClCoN_4O_2$ (249.95) C: 9.61, H 3.23, N: 22.42. Found C: 9.65, H: 3.25, N: 22.40%. FT-IR (ATR): υ /cm^{-1}: 1640, 1420, 1020, 860, 660. FT-Raman (crystal): υ /cm^{-1}: 3250, 370, 245, 95.

2.3. X-ray Crystallography

Diffraction data of single crystal was collected at 100(1) K at the Swiss-Norwegian Beamlines (SNBL) at the European Synchrotron Radiation Facility (ESRF), Grenoble, France at a wavelength of 0.798 Å. The crystal structure has been solved by dual space direct methods using SHELXT [57] in the Orthorhombic space group *Pnma* and refined by a full-matrix least squares technique on F^2 with SHELXL-2014/7 [58]. Semi empirical absorption correction was carried out using multi-scan [59]. H atoms of the water and NH_2 groups were idealized after being located in the density maps and refined as rigid groups able to rotate around the parent atom. The remaining H atoms were positioned geometrically and refined in riding. Selected crystal parameters, refinement results, bond lengths and angles are presented in Tables 1 to 3. Complete structural information was deposited with the Cambridge Crystallographic Data Center (CCDC number 2191034).

2.4. Antimicrobial Activity

The antimicrobial activity of the title compound and the ligand was evaluated by the agar diffusion method [60,61] against the following multi-resistant microorganisms: three Gram-positive bacterial strains, *Staphylococcus aureus*, *Enterococcus feacalis* (MK584170), and *Bacillus cereus* (NR074540.1), two Gram-negative bacterial strains: *Escherichia fergusonii* (MK584171), *Escherichia coli* (DH5α), and two yeast strains: *Candida sake* (MK599150) and *Candida parapsilosis* (MK599151). The strains were selected for their pathological impact and their significant resistance to antimicrobial agents and were derived from the microbial collections of the Laboratory of Microorganisms and Active Biomolecules (LMBA), Faculty of Sciences of Tunis. The bacterial strains and the two yeast strains were cultured for 18 h and 48 h respectively at 37 °C. The compounds were dissolved in aqueous medium containing 5% EtOH. The tests were carried out at two concentrations of 2.50 and 1.25 mg/mL. 70 µL of each sample was introduced into the bore agar well and incubated for 24 h at 37 °C. After incubation, the diameters of

the growth inhibition zones were measured in mm. Culture broth containing 5% EtOH and the culture broth alone were used as negative control. The experiments were carried out in duplicate.

2.5. DFT Calculations

In order to model the structure of the title compound, the monomolecular model $[Co(L)_2Cl_2(H_2O)_2]$ (Fig. 1) was calculated using DFT methods implemented in the Gaussian 09 program [62]. The calculations were performed using the B3LYP functional and 6-311++G(2d,2p) basis set [63,64] in the gas phase with a spin S = 3/2 for the Co(II) atoms. The molecular electrostatic potential (MEP) was calculated. The computed vibrational frequencies of the Infrared and Raman spectra were achieved using a scaling factor of 0.967 [65]. The Hirshfeld surfaces and the associated 2D fingerprint plot were calculated using Crystal Explorer 3.1 [66].

3. Results and discussion

3.1. Crystal Structure and Non-Covalent Interactions

3.1.1. Crystal Structure

The compound $^1_\infty[Co(\mu\text{-}L)(\mu\text{-}Cl)(H_2O)_2]Cl$ crystallized in the orthorhombic space group *Pnma* (Table 1) with one Co(II) ion, one 1,2-μ-κ^1,κ^1(N1,N2) coordinating 4-amino-4*H*-1,2,4-triazole ligand (Scheme 1), two coordinated water molecules, one bridging and coordinating Cl^- ion, and one Cl^- counter ion (Fig. 1) in the unit cell. The Co(II) ions are six coordinated by the two N1 and N2 nitrogen atoms (labelled N4 and N4^i) of the bridging 4-amino-1,2,4-triazole ligands, two *trans*-positioned Cl^- (Cl2, Cl2^i) ions and two oxygen atoms (O3, O3^i) of coordinated water molecules in a distorted octahedral geometry. When neglecting the triazole ligand Co(II) and Cl^- ligands form cationic chains $^1_\infty[CoCl]^+$, very similar to the $^1_\infty[CuCl]^+$ unit that has been found in the previously reported $[Cu(atrz)_2Cl]Cl{\cdot}H_2O$ [30].

Journal Pre-proofs

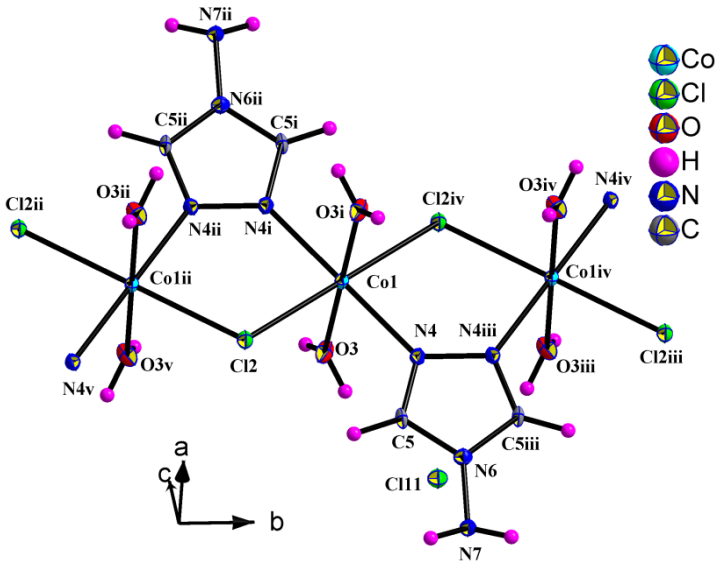


Fig. 1. View on the central structural unit of the title compound (thermal ellipsoids shown at the 50% probability level), (Symmetry code: ((i) −x+1, −y+1, −z+2; (ii) −x+1, y−1/2, −z+2; (iii) x, −y+3/2, z (iv).

Table 1. Crystallographic data for the title compound

chemical formula	$C_2H_8Cl_2CoN_4O_2$
formula weight (g·mol^{-1})	249.95
temperature (K) / crystal size	100(2) / 0.09×0.12×0.16 mm
crystal system / space group	orthorhombic / *P*nma
Cell	
a (Å)	13.3476(6)
b (Å)	7.7533(7)
c (Å)	7.3778(3)
V (Å^3) / Z	763.51(8) / 4
density calculated (Mg .m^{-3})	2.166

Journal Pre-proofs

absorption coefficient (mm^{-1})	3.97
$F(000)$	496
θ range (°) for data collection	1.7–29.9
index range	$-16 \le h \le 16$, $-7 \le k \le 7$, $-9 \le l \le 9$
reflections collected	7530
independent reflections / R_{int}	733 / 0.086
data / restraints / parameters	733 / 0 / 62
goodness-of-fit on F^2	1.1
final R indices [I>2σ(I)]	R_1: 0.038, wR_2: 0.103
CCDC	2191034

The separation of the Co atoms along the polymeric chains is 3.87(2) Å. The μ-N1,N2-bridging of the triazole leads to an almost planar five-membered N–Co–Cl–Co–N ring (Fig. 1A). The Co–Cl (2.407(8) Å) and Co–O (2.070(3) Å) bonds are relatively short, while Co–N is elongated with 2.112(4) Å, (Table 2). This is comparable with the corresponding Co–N distances in coordination polymers $Cd_{2.86}Co_{2.14}(atrz)_6(SCN)_{10}\cdot 2H_2O$ [20] and $[Co_5(atrz)_4(ox)_3(HCOO)_2]$ DMF (ox = oxalate) [23], the Co–N and Co–O distances in the trinuclear complexes $[Co_3(atrz)_6][V_6O_{18}]\cdot 3H_2O$ [41,43], $[Co_3(atrz)_6(H_2O)_6](ClO_4)_6\cdot 4.5H_2O$ [42], and $[Co_3(atrz)_6(NCS)_4(H_2O)_2](NCS)_2\cdot H_2O$ [45], and the corresponding Co–Cl, Co–O, and Co–N bond lengths reported for the dinuclear Co(II) complexes $[Co(L)Cl_2]_2$ (L = bpy, mbpy, and dmpbt) [67], $[Co(L^1)_{0.5}(5\text{-AIP})]\cdot H_2O$ (L^1 = *N,N′*-bis(3-pyridyl)oxamide; 5-H_2AIP = 5-aminoisophthalic acid), $[Co(L^3)(HBTC)]\cdot H_2O$ (L^3 = *N,N′*-di(3-pyridyl)succinamide; H_3BTC = 1,3,5-benzenetricarboxylic acid), $[Co(L^6)(HBTC)(H_2O)]\cdot 3H_2O$ (L^6 = *N,N′*-bis(3-pyridyl)sebacicdiamide), and $[Co(L^2)(1,3\text{-BDC})(H_2O)_2]$ (L^2 = *N,N′*-bis(3-pyridyl)malonamide, 1,3-H_2BDC = 1,3-benzenedicarboxylic acid) [68].

Due to the inversion symmetry, the O3–Co–O3^{i}, N4–Co–N4^{i} and Cl2–Co–Cl2^{i} angles are 180° ((i) $-x+1, -y+1, -z+2$). The O3–Co1–N4 (88.32(12)°), O3^{i}–Co1–N4 (91.68(12)°), O3–Co1–Cl2^{i} (90.25(10)°), O3^{i}–Co1–Cl2^{i} (89.75(10)°), N4–Co1–Cl2 (89.94(11)°), and N4^{i}–Co1–Cl2 angles (90.06(11)°) are all quite close to the ideal 90°. From the Co1–Cl2–Co1^{ii} ((ii) $-x+1, y-1/2, -z+2$) angle of 107.25(5)° we conclude that there is no strain in the coordination of Co(II) with the bridging Cl^- resulting from the μ,N1,N2 coordination of the ligand and the N–Co–Cl–Co–N ring.

Table 2. Selected bond lengths and angles of the title compound.[a,b]

bonds lengths (Å)	exp.	DFT-calc.	bonds lengths (Å)	exp.	DFT-calc.
Co1–O3	2.070(3)	1.964	Co1–Cl2	2.407(8)	2.370
Co1–O3^{i}	2.070(3)	1.992	N4–N4^{iii}	1.385(8)	1.383
Co1–N4	2.112(4)	1.962	C5–N6	1.338(5)	1.358
Co1–N4^{i}	2.112(4)	2.003	N6–C5^{iii}	1.338(5)	1.370
Co1–Cl2^{i}	2.407(8)	2.448	N6–N7	1.401(6)	1.400
angles (°)	exp.	DFT-calc.	angles (°)	exp.	DFT-calc.
O3–Co1–N4	88.32(12)	89.312	Cl2^{i}–Co1–Cl2	180	175.320
O3^{i}–Co1–N4	91.68(12)	91.285	O3–Co1–O3^{i}	180	176.545
O3–Co1–N4^{i}	91.68(12)	92.282	C5–N4–N4^{iii}	107.2(3)	108.335
O3^{i}–Co1–N4^{i}	88.32(12)	87.368	C5–N4–Co1	125.9(3)	129.230
N4–Co1–N4^{i}	180	175.583	N4^{iii}–N4–Co1	126.16(11)	122.434
O3–Co1–Cl2^{i}	90.25(10)	87.664	N4–C5–N6	109.3(4)	108.761
O3^{i}–Co1–Cl2^{i}	89.75(10)	95.780	C5^{iii}–N6–C5	107.0 (5)	106.630
N4–Co1–Cl2^{i}	89.94(11)	84.073	C5^{iii}–N6–N7	126.5 (2)	129.444
N4^{i}–Co1–Cl2^{i}	90.06(11)	91.873	C5–N6–N7	126.5 (2)	123.920

[a]) Symmetry codes: (i) −x+1, −y+1, −z+2; (ii) −x+1, y−1/2, −z+2; (iii) x, −y+3/2, z. [b)] DFT calculations using the B3LYP functional and 6-311++G(2d,2p) basis set on the mononuclear model $[Co(L)_2Cl_2(H_2O)_2]$.

3.1.2. Non-Covalent Interactions

A common approach to the study of crystal supramolecular architectures is to analyze all forms of non-covalent interactions like conventional (O(N)–H···O and O(N)–H···Cl) and unconventional (C–H···O(Cl) and C–H···π) hydrogen bonds, halogen bonds, stacking interactions and van der Waals interactions [69,70]. In the here presented structure, the polymeric 1D chains were held together by an extended N–H···O (N7–H7···O3^{v}) and O–H···Cl (O3–H3A···Cl11^{iv} and O3–H3B···Cl11^{iv}) hydrogen bridging network with strong contributions from the 4-amino group or the triazole ligand, the coordinated water molecules and the Cl^- (Cl11) counter ion (Fig. 2). Overall, the A···H and D···A distances cover a range from 2.233 Å to 2.696 Å and 3.122 Å to 3.566 Å respectively (Table 3) and are thus assigned to weak hydrogen bonds [71,72]. Similar hydrogen bonds were previously reported for the dinuclear Co(II) complex $[Co_2(Hatzc)_2(H_2O)_6](NO_3)_2{\cdot}4H_2O$ ($Hatzc^-$ = 3-amino-4*H*-1,2,4-triazole-5-carboxylate) [73], Zn(II) coordination polymers with 3-amino-1,2,4-triazole [74], and $[MnCl_3(H_2O)_2(Hatz)]{\cdot}H_2O$ (Hatz = 3-amino-1,2,4-triazole) [75], while in the end-on N1-binding 1-vinyl-3-acetylamino-1,2,4-triazole (vaat) containing compounds $[Ni(vaat)_2(H_2O)_2](NO_3)_2$ and $[Cu(vaat)_2(H_2O)_2]Cl_2$ no such hydrogen bonds were observed [76].

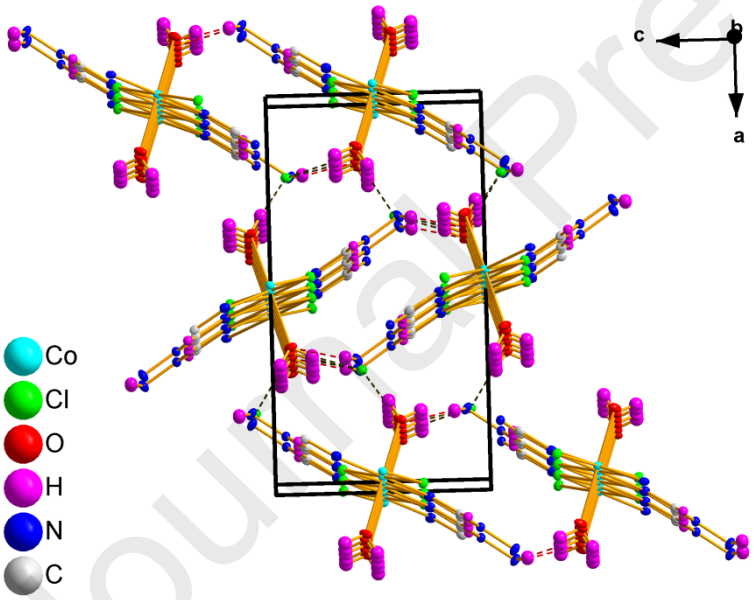


Fig. 2. View of the crystal packing for $^{1}_{\infty}[Co(\mu\text{-}L)(\mu\text{-}Cl)(H_2O)_2]Cl$ showing the hydrogen bonds N–H···O (dashed red lines) and O–H···Cl (dashed green lines).

Table 3. Selected hydrogen bonds for $^{1}_{\infty}[Co(\mu\text{-}L)(\mu\text{-}Cl)(H_2O)_2]Cl$.

D–H···A	D–H (Å)	H···A (Å)	D···A (Å)	<(DHA)> (°)

O3–H3A···Cl11^{iv}	0.820	2.366	3.125(2)	154.29
O3–H3B···Cl11^{iv}	0.820	2.336	3.122(2)	160.89
N7–H7···O3^{v}	0.860	2.233	3.127(2)	153.73
C5–H5···Cl11^{iv}	0.950	2.696	3.566(2)	152.53
C5–H5···Cl2	0.950	2.662	3.212(2)	117.39

Symmetry codes: (iv) –x+1/2, –y+1, z+1/2, (v) x, –y+3/2, z–1.

The Hirshfeld surface was calculated and mapped over a d_{norm} confirming the intermolecular interactions in addition to the Van der Waals interactions (Fig. S1 in the Supplementary Materials). The calculation shows a volume of the voids of approximately 18 Å^3 which makes about 7% of the cell volume and the surface area equal to 114 Å^2. However, the voids are very probably not accessible and thus of virtual nature.

The 2-D fingerprint plots (Fig. S2) show that the H···H contacts cover 42.2% of the total surface followed by the Cl···H/H···Cl contacts with 23.9%. Minor contributions come from N···H/H···N (7%), Cl···N/N···Cl (6.7%), O···N/N···O (2.8%), and O···H/H···O (2.7%) contacts in good agreement with the multiple N–H···O and O–H···Cl hydrogen bonding interactions.

3.2. DFT-Geometry Optimization and Molecular Electrostatic Potential (MEP)

The DFT-calculated optimized geometry of the monomolecular model $[Co(L)_2Cl_2(H_2O)_2]$ and the metrical data obtained from X-ray diffraction of the title compound show a good agreement (Table 2, Fig. 3a). MEP surface calculations were performed in order to investigate the reactive sites of the title compound. The red (negative) region is corresponding to the most nucleophilic sites, while the blue (positive) region represents to the most electrophilic sites. The analysis of (Fig. 3b) shows that the chloride and oxygen atoms are the most nucleophilic sites with a $v_{S\ min}$ equal to –35.14 and –19.45 kcal·mol^{-1}, respectively. The most electrophilic site is attributed to the hydrogen atoms linked to the nitrogen atoms with a $v_{S\ max}$ equal to 39.53 kcal·mol^{-1}.

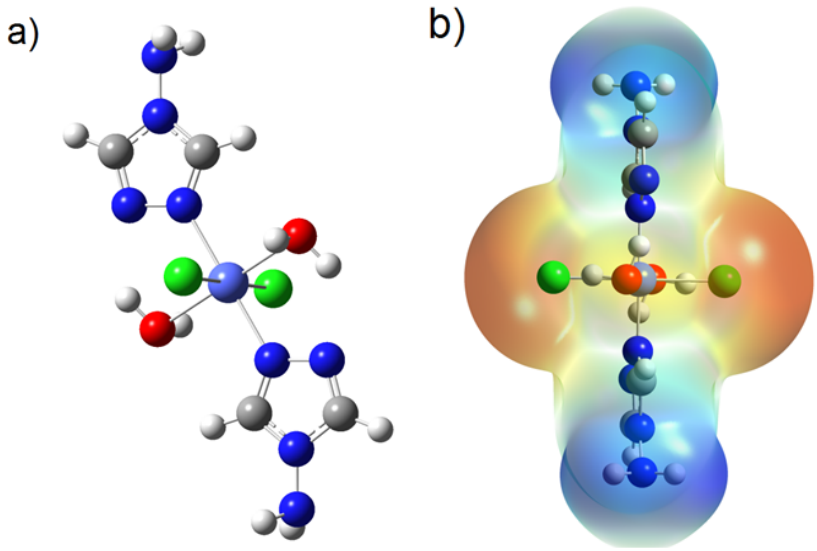


Fig. 3. The DFT-optimized geometry (a) and molecular electrostatic potential (MEP) (b) of the monomolecular model $[Co(L)_2Cl_2(H_2O)_2]$.

3.3. Vibrational Spectroscopy

The experimental IR spectrum (Fig. S3) showed a broad envelope from 3700 to 2300 cm^{-1} with maxima at 3270, 3200 and 3080 cm^{-1} which can be assigned to N–H, O–H and C–H stretching modes [73–78]. The DFT-calculated IR spectrum showed two strong bands at 3540 and 3525 cm^{-1} assigned to the O-H stretching modes of the coordinated water molecules. Thus, these two intense calculated bands have no strong experimental counterpart, which might be due to the monomolecular model $[Co(L)_2Cl_2(H_2O)_2]$ that has been used for the calculations. In contrast to this, the N–H and C–H stretches were calculated at 3280 and 3130 cm^{-1} in agreement with the experimental maxima. The experimentally observed bands at 1640, 1420 and 1020 cm^{-1} were attributed to the C=N, C–N and N–N stretching modes of the triazole [73,77–80]. The calculation predicts these bands at 1645, 1455 and 1005 cm^{-1} respectively in good agreement. The strong bands observed at 860 and 660 cm^{-1} were attributed to the (O–H) and (C–H) bending modes respectively [73]. The calculation predicts these bands at 880 and 670 cm^{-1} respectively in very good agreement with the experimental data.

In the experimental Raman spectrum (Fig. S4), the same broad envelope as in the IR spectrum from 3400 to 2500 cm^{-1} with one pronounced peak at 3250 cm^{-1} was observed and attributed to the O–H, N–H and C–H stretching modes [73,78,80].

The DFT-calculated values of these stretching modes are at 3530, 3520, 3370, 3320, and 3005 cm^{-1} respectively, thus in good agreement with the experimental data. As for the IR, the agreement of the DFT-calculated data in the range 1650 to 550 cm^{-1} is not perfect. In the low frequency range 400 to 20 cm^{-1}, the peaks observed at 370, 245 and 95 cm^{-1} are assigned to the Co–N, Co–O and Co–Cl stretching modes [73,81]. The DFT-calculation predicts these bands at 390, 250 and 110 cm^{-1} respectively in excellent agreement with the experimental data.

As expected, for both Raman and IR spectra, the DFT-calculated data shows lacking agreement with the experimental data on those motions (modes) that are connected to the extensive hydrogen bonding in the crystal. The same is true for some of the modes assignable to the triazole ligand,

especially the N–N stretch. The monomolecular model $[Co(L)_2Cl_2(H_2O)_2]$ with monodentate bound triazole, calculated in the gas phase could barely account for these interactions. In contrast, vibrational modes centered around the Co(II) atom were reproduced by the DFT calculation with high accuracy.

3.4. Thermal Analysis

The TGA curve shows six distinct weight loss steps (Fig. S5). The first in the range between 100 and 180 °C is related to an endothermic peak in the DSC curve and can be assigned to the loss of the two coordinated water molecules (experimental and calculated weight loss is 14.1%). The second and third weight loss steps of the TGA curve occurred in the range of 230 to 320 °C and 325 to 380 °C respectively and are connected with two exothermic peaks in the DSC curve. They can be attributed to the loss of the two chloride atoms in the form of HCl. The calculated residue $C_2H_2CoN_4$ makes 56.64% percent of the original mass, which is in excellent agreement with the experimental value. The organic ligand starts to decompose at 385 °C, finally leaving a residue of less than 20%. The DSC shows several exothermic peaks in this region in line with a complex decomposition. If we assume elemental Co as the remainder, the final mass should be 23.6% of the original mass. We suspect that evaporation of volatile species adds to the mass loss starting from about 700 °C. Mass spectrometry recorded during the composition (Fig. S6) confirmed the assignments.

3.5. Antimicrobial Activity

The evaluation of the antimicrobial activity using the agar diffusion method showed that the title compound inhibits five microbial strains with diameters of inhibition zone ranging between 10 and 20 mm at 1.25 and 2.5 mg/mL (Fig. 4 and Fig. S7). The highest activities were found against the Gram-negative *E. fergusonii* and the yeast *C. parapsilosis* slightly while lower activities were found for the Gram-positive bacteria *S. aureus*, *E. feacalis*, and *B. cereus*. In contrast to this, no inhibitory activity was detected against the Gram-negative *E. coli* and yeast *C. sake*. For the ligand, no inhibitory activity was found at 2.5 mg/mL.

Journal Pre-proofs

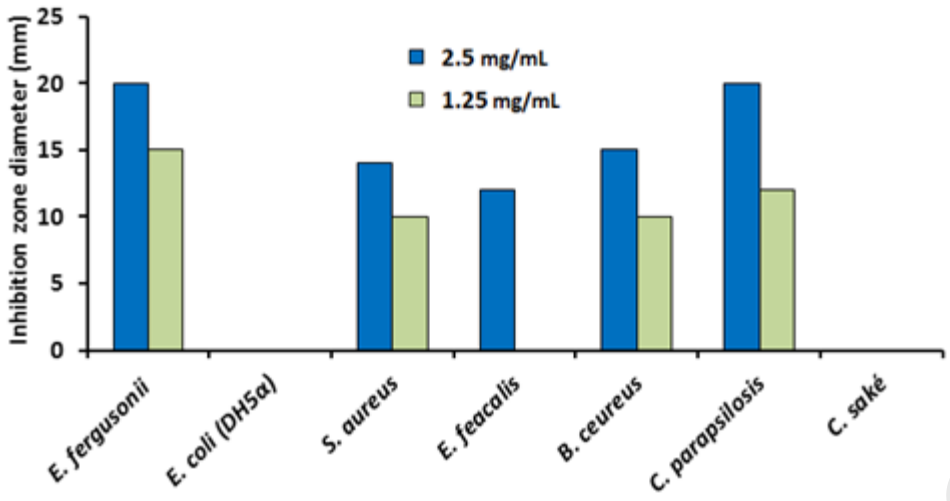


Fig. 4. Inhibition diameters zones (mm) at concentrations of 1.25 and 2.50 mg/mL after 24 h.

The activity against *S. aureus* is an exciting result of our study as *S. aureus* is one of the most problematic bacterial strains in clinical medicine with the emergence of antibiotic-resistant strains such as methicillin-resistant *S. aureus* (MRSA). Similar results were observed for the compounds $[Co(dmtp)_2(OH_2)_4][CoCl_4]$ and $[Co(dmtp)_2(OH_2)_4]Cl_2{\cdot}2H_2O$ (dmtp = 5,7-dimethyl-1,2,4-triazolo[1,5-a]pyrimidine) [82], which showed comparable antibacterial activity against *S. aureus*. As one of the established drugs against MRSA, vancomycin a typical glycopeptide antibiotic, showed inhibition zones of 11 to 16 mm at a minimum inhibitory concentration (MIC) of 0.125 μg/mL for selected methicillin-resistant *S. aureus* strains and only 0.5 μg/mL for a huge number of strains in clinic experiments [83], while MICs of 4 μg/mL were very recently reported for linezolid ((*S*)-*N*-({3-[3-fluor-4-(4-morpholinyl)phenyl]-2-oxo-5-oxazolidinyl}methyl)acetamid) [84]. Thus, the MICs of such organic drugs lie about 10 times lower than our Co(II) compound.

On the other hand, we are far from being able to rationalize the peculiar observed selectivity of the here studied Co(II) compound which calls for further in-depths studies, including cell-viability tests. Furthermore, although the stability of the pink color of the test solutions clearly shows the stability of the Co(II) oxidation state of the species in solution, we are less sure about the size of the species. From the virtually unchanged color we assume that the polymeric character is retained. However, we cannot exclude the formation of oligomers. Also this aspect will be studied in the future.

4. Conclusions

A new Co(II) coordination polymer $^1{}_\infty[Co(\mu\text{-}L)(\mu\text{-}Cl)(H_2O)_2]Cl$ based on 4-amino-1,2,4-triazole was synthesized from $CoCl_2{\cdot}6H_2O$ and 4-amino-4*H*-1,2,4-triazole (atrz). Single crystal X-ray diffraction showed that the Co(II) ions are coordinated by the N1 and N2 atoms of the bridging 4-amino-1,2,4-triazole ligand, two *trans*-oriented bridging Cl^- ligands and two O atoms from coordinated water molecules in a distorted octahedral geometry. Hirshfeld surface analysis confirmed that the structure

is dominated by N–H···O and O–H···Cl hydrogen bonds interactions. The theoretical FT-IR and FT-Raman spectra of the title compound have been calculated, which show *good* agreement with recorded spectra. Thermal analysis (TGA and DSC) shows that the title compound is stable up to 100 °C, a temperature that corresponds to the loss of water molecules. The compound is also is remarkably stable in solution exposed to air and conserves its oxidation state Co(II) as well as its coordination. An in vitro antimicrobial study using the agar diffusion method showed high activities against the Gram-negative *E. fergusonii* and the yeast *C. parapsilosis* and slightly reduced activities against the the Gram-positive and notoriously antibiotic-resistant bacteria *S. aureus*, *E. feacalis*, and *B. cereus*. No activity was found against *E. coli* bacteria and the yeast *C. saké*. In future work, we aim to provide more detailed information on the interaction of the compound (or its metabolic products) with biological material. Overall, metal complexes based on 4-amino-1,2,4-triazole can play an important role in the development of new drugs.

Declaration of Competing Interest

There are no competing interests to declare.

Acknowledgements

Financial support from the Ministry of Higher Education and Scientific Research of Tunisia is gratefully acknowledged. The authors are grateful to the University of Tunis El Manar for funding. Souhir Sallemi and Hadda-Imene Ouzari, University of Tunis El Manar, Faculty of Sciences of Tunis, Laboratory of Microorganisms and Active Biomolecules (LMBA-LR03ES03), 2092 El Manar II, Tunis, are thanked for the antimicrobial tests. Eric Tobechukwu Anthony, University of Cologne, Department of Chemistry is acknowledged for help with the revision.

Appendix A. Supplementary Materials

Supplementary material to this article can be found online at https://doi.org/10.1016/j.ica.

References

[1] G. Arroyos, C.M. da Silva, L.B. Theodoroviez, J.E.M. Campanella, R.C.G. Frem, Insights on Luminescent Micro- and Nanospheres of Infinite Coordination Polymers, Chem.–Eur. J. 28 (2022) e202103104 (1–19). DOI: 10.1002/chem.202103104

[2] S.S. García-R. Solórzano, R. Alibés, F. Busqué, F. Novio, D.R. Molina, Coord. Chem. Rev. 441 (2021) 213977. DOI: 10.1016/j.ccr.2021.213977

[3] K. Biradha, A. Goswami, R. Moi, Coordination polymers as heterogeneous catalysts in hydrogen evolution and oxygen evolution reactions, Chem. Commun. 56 (2020) 10824–10842. DOI: 10.1039/d0cc04236f

[4] R. Kretschmer, Ligands with Two Monoanionic N,N-Binding Sites: Synthesis and Coordination Chemistry, Chem.–Eur. J. 26 (2020) 2099–2119. DOI: 10.1002/chem.201903442

[5] J. Conesa-Egea, F. Zamora, P. Amo-Ochoa, Perspectives of the smart Cu-Iodine coordination polymers: A portage to the world of new nanomaterials and composites, Coordination Chemistry Reviews 381 (2019) 65–78. DOI: 10.1016/j.ccr.2018.11.008

[6] Q. Yue, E.-Q. Gao, Azide and carboxylate as simultaneous coupler for magnetic coordination polymers, Coord. Chem. Rev. 382 (2019) 1–31. DOI: 10.1016/j.ccr.2018.12.002

[7] E. San Sebastian, A. Rodríguez-Diéguez, J. M. Seco, J. Cepeda, Coordination Polymers with Intriguing Photoluminescence Behavior: The Promising Avenue for Greatest Long-Lasting Phosphors, Eur. J. Inorg. Chem. 2018 (2018) 2155–2174. DOI: 10.1002/ejic.201800124

[8] R.F. D'Vries, G.E. Gomez, J. Ellena, Highlighting Recent Crystalline Engineering Aspects of Luminescent Coordination Polymers Based on F-Elements and Ditopic Aliphatic Ligands. Molecules 27 (2022) 3830. DOI: 10.3390/molecules27123830

[9] C.E. Housecroft, E.C. Constable, The terpyridine isomer game: from chelate to coordination network building block, Chem. Commun. 56 (2020) 10786–10794. DOI: 10.1039/d0cc04477f

[10] M. Li, D. Li, M. O'Keeffe, O.M. Yaghi, Topological Analysis of Metal−Organic Frameworks with Polytopic Linkers and/or Multiple Building Units and the Minimal Transitivity Principle, Chem. Rev. 114 (2014) 1343−1370. DOI: 10.1021/cr400392k

[11] W. Ouellette, S. Jones, J. Zubieta, Solid state coordination chemistry of metal-1,2,4-triazolates and the related metal-4-pyridyltetrazolates, CrystEngComm. 13 (2011) 4457–4485. DOI: 10.1039/C0CE00919A

[12] G. Aromí, L.A. Barrios, O. Roubeau, P. Gamez, Triazoles and tetrazoles: Prime ligands to generate remarkable coordination materials, Coord. Chem. Rev. 255 (2011) 485–546. DOI: 10.1016/j.ccr.2010.10.038

[13] U. Beckmann, S. Brooker, Cobalt(II) complexes of pyridazine or triazole containing ligands: spin-state control, Coord. Chem. Rev. 245 (2003) 17–29. DOI: 10.1016/S0010-8545(03)00030-4

[14] P. Wu, Q. Xue, X. Dong, Y. Zhang, H. Hu, B. Liu, G. Xue, Three Organic–Inorganic Hybrids Based on [MoxOy]n– Chains Decorated with Organic Ligands and Transition-Metal Coordination Complexes, Eur. J. Inorg. Chem. 2017 (2017) 3516–3524. DOI: 10.1002/ejic.201700441

[15] U. Garcia-Couceiro, D. Olea, O. Castillo, A. Luque, P. Roman, P.J. de Pablo, J. Gomez-Herrero, F. Zamora, Scanning Probe Microscopy Characterization of Single Chains Based on a One-Dimensional Oxalato-Bridged Manganese(II) Complex with 4-Aminotriazole, Inorg. Chem. 44 (2005) 8343–8348. DOI: 10.1021/ic0505302

[16] R.F. Lonergan, G.A. Conway, P.W. Doheny, H.J. Shepherd, Spontaneous Synthesis of $[Fe^{II}(Atrz)_3]SO_4$ and its Analogues Through Accelerated Ageing: New Insights from Small-Scale Reactions, Chem. Eur. J. 28 (2022) e202201823 (1–10). DOI: 10.1002/chem.202201823

[17] V. Kumar, A. Rotarub, Y. Garcia, Room temperature light induced spin state switching in a Fe^{II} coordination polymer featuring a photo responsive anion, J. Mater. Chem. C 10 (2022) 14128–14134. DOI: 10.1039/d2tc02415b

[18] A. Enriquez-Cabrera, L. Getzner, L. Salmon, L. Routaboul, A. Bousseksou, Post-synthetic modification mechanism for 1D spin crossover coordination polymers, New J. Chem. 46 (2022) 22004–22012. DOI: 10.1039/d2nj04015h

[19] I. Bräunlich, A. Sánchez-Ferrer, M. Bauer, R. Schepper, P. Knüsel, J. Dshemuchadse, R. Mezzenga, W. Caseri, Polynuclear Iron(II)−Aminotriazole Spincrossover Complexes (Polymers) In Solution, Inorg. Chem. 53 (2014) 3546−3557. DOI: 10.1021/ic403035u

[20] Y.-T. Gou, F. Yue, H.-M. Chen, G. Liu, D.-C. Sun, Syntheses and Structures of 3d-4d Heterometallic Coordination Polymers Based on 4-Amino-1,2,4-triazole, J. Coord. Chem. 66 (2013) 1889-1896. DOI: 10.1080/00958972.2013.794384

[21] J. Bao, X. Li, J. Wang, Y. Cong, J. Zhou, X. Zhang, W. Chen, Crystallization, morphology and mechanical property enhancement of block copolymer-based metallosupramolecular polymers by incorporating metal coordinating ligand into poly(*L*-lactic acid) block, Polymer 256 (2022) 125191. DOI: 10.1016/j.polymer.2022.125191

[22] Y. Zhao, M. Yang, S. Rong, X. Wang, H. Ma, H. Pang, L. Tan, K. Gao Polyoxotungstates-supported Ni^{II}/Co^{II}-containing 3D inorganic-organic hybrids as supercapacitor electrodes toward boosting capacitor performance, J. Electroanal. Chem. 882 (2021) 115017. DOI: 10.1016/j.jelechem.2021.115017

[23] J.-J. Hou, X. Xu, N. Jiang, Y.-Q. Wu, X.-M. Zhang, Selective adsorption in two porous triazolate–oxalate-bridged antiferromagnetic metal-azolate frameworks obtained via in situ decarboxylation of 3-amino-1,2,4-triazole-5-carboxylic acid, J. Solid State Chem. 223 (2015) 73–78. DOI: 10.1016/j.jssc.2014.06.016

[24] M. M. Dîrtu, Y. Garcia, B. Tinant, Structures of new Cu(II) and Co(II) 4-amino-1,2,4-triazole coordination compounds, Acta Cryst. (2006). A62, s275.

[25] H. Li, Y. Wang, Z. Wei, X. Yang, L. Liang, L. Xia, M. Long, Z. Li, T. Zhang, Tunable copper complexes with functional ligands: A promising strategy for green primary explosives, Chem. Engin. J. 430 (2022) 132739. DOI: 10.1016/j.cej.2021.132739

[26] E.-C. Yang, Z.-Y. Liu, S.-H. Chen, Y.-H. Su, Y.-Y. Zhang, X.-J. Zhao, Four linear Cu^{II}_3 subunit-based coordination polymers with various inter-subunit connections, spin ground-states and intra-/inter-subunit magnetic couplings, Dalton Trans. 44 (2015) 3190–3199. DOI: 10.1039/c4dt03741c

[27] X.-L. Wang, C.-H. Gong, J.-W. Zhang, G.-C. Liu, X.-M. Kan, N. Xu, Polyoxometalate-directed assembly of various multinuclear metal–organic complexes with 4-amino-1,2,4-triazole and selective photocatalysis for organic dye degradation, CrystEngComm. 17 (2015) 4179–4189. DOI: 10.1039/c5ce00411j

[28] P.-N. Wang, C.-W. Yeh, C.-H. Tsou, Y.-W. Ho, H.-T. Lee, M.-C. Suen, Structural diversity in Cu(II) and Cd(II) coordination complexes with 4-amino-1,2,4-triazole ligand, Inorg. Chem. Commun. 43 (2014) 70-74. DOI: 10.1016/j.inoche.2014.02.002

[29] Y.-Y. Zhang, Q. Liu, E.-C. Yang, X.-J. Zhao, Three new coordination polymers with tetranuclear cluster-based 3D framework and bent 1D ribbons generated from ternary copper(II)-triazole-citrate system: Synthesis, structure, and magnetism, Inorg. Chim. Acta 415 (2014) 81–87. DOI: 10.1016/j.ica.2014.02.029

[30] M.M. Dîrtu, Y. Boland, D. Gillard, B. Tinant, K. Robeyns, D.A. Safin, E. Devlin, Y. Sanakis, Y. Garcia, New Mononuclear Cu(II) Complexes and 1D Chains with 4-Amino-4*H*-1,2,4-triazole, Int. J. Mol. Sci. 14 (2013) 23597–23613. DOI: 10.3390/ijms141223597

[31] S. Cudziło, M. Nita, Synthesis and explosive properties of copper(II) chlorate(VII) coordination polymer with 4-amino-1,2,4-triazole bridging ligand, J. Hazard. Mater. 177 (2010) 146–149. DOI: 10.1016/j.jhazmat.2009.12.008.

[32] M. Yang, S. Rong, X. Wang, H. Ma, H. Pang, L. Tan, Y. Jiang, K. Gao, Preparation and Application of Keggin Polyoxometalate-based 3D Coordination polymer Materials as Supercapacitors and Amperometric Sensors, ChemNanoMat. 7 (2021) 299–306. DOI: 10.1002/cnma.202000654

[33] A.-X. Zhu, Q.-Q. Xu, F.-Y. Liu, Z. Li, X.-L. Qi, Syntheses, crystal structures and luminescent properties of copper(I)-halide complexes constructed by 4-amino-3,5-dimethyl-1,2,4-triazole, Inorg. Chim. Acta 370 (2011) 333–339. DOI: 10.1016/j.ica.2011.01.090

[34] F.A. Mautner, C. Berger, C. Gspan, B. Sudy, R.C. Fischer, S.S. Massoud, Pyridyl and triazole ligands directing the assembling of zinc(II) into coordination polymers with different dimensionality through azides, Polyhedron 130 (2017) 136-144. DOI: 10.1016/j.poly.2017.04.012

[35] S.-H. Zhang, J.-M. Wang, H.-Y. Zhang, Y.-P. Fan, Y. Xiao, Highly efficient electrochemiluminescence based on 4-amino-1,2,4-triazole Schiff base two-dimensional Zn/Cd coordination polymers, Dalton Trans. 46 (2017) 410–419. DOI: 10.1039/c6dt04059d

[36] M. Said, H. Boughzala, A new cadmium coordination polymer based on 4-amino-4H-1,2,4-triazole, Acta Crystallogr., Sect. E: Crystallogr. Commun. E74 (2018) 147–150. DOI: 10.1107/S2056989018000464

[37] Y. Gong, T. Wu, P.G. Jiang, J.H. Lin, Y.X. Yang, Octamolybdate-Based Metal–Organic Framework with Unsaturated Coordinated Metal Center As Electrocatalyst for Generating Hydrogen from Water, Inorg. Chem. 52 (2013) 777–784. DOI: 10.1021/ic3018858

[38] Q.-L. Wang, H. Xu, H.-W. Hou, G. Yang, Synthesis and Structures of Silver(I) Adducts with 4-Amino-4*H*-1,2,4-triazole, Z. Naturforsch. 64b (2009) 1143–1146. DOI: 10.1515/znb-2009-1006

[39] L. Váhovská, O. Bukrynov, I. Potočňák, E. Čižmár, A. Kliuikov, S. Vitushkina, M. Dušek, R. Herchel, New Cobalt(II) Field-Induced Single-Molecule Magnet and the First Example of a Cobalt(III) Complex with Tridentate Binding of a Deprotonated 4-Amino-3,5-bis(pyridin-2-yl)-1,2,4-Triazole Ligand, Eur. J. Inorg. Chem. 2019 (2019) 250–261, DOI: 10.1002/ejic.201801225

[40] W. A. Jawad, A. A. A. Al-Hussein Balakit, M. N. A. Al-Jibouri, Synthesis, Characterization and Antibacterial Activity Study of Cobalt(II), Nickel(II), Copper(II), Palladium(II), Cadmium(II) and Platinum(IV) Complexes with 4-Amino-5-(3,4,5-trimethoxyphenyl)-4H-1,2,4-triazole-3-thione, Indon. J. Chem. 21 (2021) 1514–1525. DOI: 10.22146/ijc.67021

[41] J. Li, C. Wei, Y Han, Y. Mei, X. Cheng, X. Huang, C. Hu, Triazole-directed fabrication of polyoxovanadate-based metal–organic frameworks as efficient multifunctional heterogeneous catalysts for the Knoevenagel condensation and oxidation of alcohols, Dalton Trans. 50 (2021) 10082–10091. DOI: 10.1039/d1dt01413g

[42] C. Xu, J. Zhang, X. Yin, Z. Cheng, Structural Diversity and Properties of M(II) Coordination Compounds Constructed by 3-Hydrazino-4-amino-1,2,4-triazole Dihydrochloride as Starting Material, Inorg. Chem. 55 (2016) 322–329. DOI: 10.1021/acs.inorgchem.5b02434

[43] X.-L. Wang, C.-H. Gong, J.-W. Zhang, L.-L. Hou, J. Luan, G.-C. Liu, Substituent position-induced diverse architectures of polyoxovanadate-based hybrid materials constructed from a linear trinuclear transition metal complex and a hexanuclear $[V_6O_{18}]^{6-}$ cluster, CrystEngComm. 16 (2014) 7745–7752. DOI: 10.1039/c4ce00988f

[44] H.S. Yoo, J.H. Lim, J.S. Kang, E.K. Koh, C.S. Hong, Triazole-bridged magnetic M(II) assemblies (M = Co, Ni) capped with the end-on terephthalate dianion involving multi-intermolecular contacts, Polyhedron 26 (2007) 4383–4388. DOI: 10.1016/j.poly.2007.05.051

[45] Y.-Q. Huang, B. Ding, H.-L. Gao, P. Cheng, D.-Z. Liao, S.-P. Yan, Z.-H. Jiang, Syntheses, structures and characterization of novel cobalt(II) mono- and bi-triazole complexes, J. Mol. Struct. 743 (2005) 201–207. DOI: 10.1016/j.molstruc.2005.03.010

[46] M.H. Klingele, B. Moubaraki, K.S. Murray, S. Brooker, Synthesis and Some First-Row Transition-Metal Complexes of the 1,2,4-Triazole-Based Bis(terdentate) Ligands TsPMAT and PMAT, Chem.–Eur. J. 11 (2005) 6962–6973. DOI: 10.1002/chem.200500387

[47] U. García-Couceiro, O. Castillo, A. Luque, J.P. García-Terán, G. Beobide, P. Román, One-Dimensional Oxalato-Bridged Metal(II) Complexes with 4-Amino-1,2,4-triazole as Apical Ligand, Eur. J. Inorg. Chem. 2005 (2005) 4280–4290. DOI: 10.1002/ejic.200500332

[48] L. G. Lavrenova, S. V. Larionov, S. A. Grankina, Complexes of metals with 4-amino-1,2,4-triazole, Izv. Sib. Otd. Akad. Nauk SSSR, Ser. Khim. Nauk 5 (1979) 88–92.

[49] M. Das, B. Das, A. Samanta, Antioxidant and anticancer activity of synthesized 4-amino-5-((aryl substituted)-4*H*-1,2,4-triazole-3-yl)thio-linked hydroxamic acid derivatives, J. Pharm. Pharmacol. 71 (2019) 1400–1411. DOI: 10.1111/jphp.13131

[50] I. Saadaoui, F. Krichen, B.B. Salah, R.B. Mansour, N. Miled, A, Bougatef, M. Kossentini, Design, synthesis and biological evaluation of Schiff bases of 4-amino-1,2,4-triazole derivatives as potent angiotensin converting enzyme inhibitors and antioxidant activities, J. Mol. Struct. 1180 (2019) 344–354. DOI: 10.1016/j.molstruc.2018.12.008

[51] S. Tariq, P. Kamboj, O. Alam, M. Amir, 1,2,4-Triazole-based benzothiazole/benzoxazole derivatives: Design, synthesis, p38α MAP kinase inhibition, anti-inflammatory activity and molecular docking studies, Bioorg. Chem. 81 (2018) 630–641. DOI: 10.1016/j.bioorg.2018.09.015

[52] N. Süleymanoğlu, Y. Ünver, R. Ustabaş, Ş. Direkel, G. Alpaslan, Antileishmanial activity study and theoretical calculations for 4-amino-1, 2, 4-triazole derivatives, J. Mol. Struct. 1144 (2017) 80–86. DOI: 10.1016/j.molstruc.2017.05.017

[53] E. Düğdü, Y. Ünver, D. Ünlüer, K. Sancak, Synthesis and Biological Properties of Novel Triazole-Thiol and Thiadiazole Derivatives of the 1,2,4-Triazole-3(5)-one Class, Molecules 19 (2014) 2199–2212. DOI: 10.3390/molecules19022199

[54] Z.H. Chohan, M. Hanif, Design, synthesis, and biological properties of triazole derived compounds and their transition metal complexes, J. Enzyme Inhib. Med. Chem. 25 (2010) 737–749. DOI: 10.3109/14756360903389906

[55] H. Bayrak, A. Demirbas, S.A. Karaoglu, N. Demirbas, Synthesis of some new 1,2,4-triazoles, their Mannich and Schiff bases and evaluation of their antimicrobial activities, Eur. J. Med. Chem. 44 (2009) 1057–1066. DOI: 10.1016/j.ejmech.2008.06.019

[56] B.S. Holla, R. Gonsalves, S. Shenoy, Synthesis and antibacterial studies of a new series of 1,2-bis(1,3, 4-oxadiazol-2-yl)ethanes and 1,2-bis(4-amino-1,2,4-triazol-3-yl)ethanes, Eur. J. Med. Chem. 35 (2000) 267−271. DOI: 10.1016/S0223-5234(00)00154-9

[57] G.M. Sheldrick, SHELXT – Integrated space-group and crystal-structure determination, Acta Cryst. A: Found. Adv. 71 (2015) 3–8. DOI: 10.1107/S2053273314026370

[58] G.M. Sheldrick, SHELXL-2014, Program for the Refinement of Crystal Structures University of Göttingen, Göttingen, Germany (2014).

[59] G.M. Sheldrick, SADABS (Version 2.03), University of Gottingen, Germany (2002).

[60] N.G. Heatley, A method for the assay of penicillin, Biochem. J. 38 (1944) 61–65. DOI: 10.1042/bj0380061

[61] Clinical and Laboratory Standards Institute, Method for Antifungal Disk Diffusion Susceptibility Testing of Yeasts, Approved Guideline. CLSI document M44-A. CLSI, 940 West Valley Road, Suite 1400, Wayne, PA, 19087-1898, USA, (2004).

[62] Gaussian 09, Revision A.1, M.J. Frisch, G.W. Trucks, H.B. Schlegel, G.E. Scuseria, M.A. Robb, J.R. Cheeseman, G. Scalmani, V. Barone, B. Mennucci, G.A. Petersson, H. Nakatsuji, M. Caricato, X. Li, H.P. Hratchian, A.F. Izmaylov, J. Bloino, G. Zheng, J.L. Sonnenberg, M. Hada, M. Ehara, K. Toyota, R. Fukuda, J. Hasegawa, M. Ishida, T. Nakajima, Y. Honda, O. Kitao, H. Nakai, T. Vreven, J.A. Montgomery, Jr., J.E. Peralta, F. Ogliaro, M. Bearpark, J.J. Heyd, E. Brothers, K.N. Kudin, V.N. Staroverov, R. Kobayashi, J. Normand, K. Raghavachari, A. Rendell, J.C. Burant, S.S. Iyengar, J. Tomasi, M. Cossi, N. Rega, J.M. Millam, M. Klene, J.E. Knox, J.B. Cross, V. Bakken, C. Adamo, J. Jaramillo, R. Gomperts, R.E. Stratmann, O. Yazyev, A.J. Austin, R. Cammi, C. Pomelli, J.W. Ochterski, R.L. Martin, K. Morokuma, V.G. Zakrzewski, G.A. Voth, P. Salvador, J.J. Dannenberg, S. Dapprich, A.D. Daniels, O. Farkas, J.B. Foresman, J.V. Ortiz, J. Cioslowski, J. Fox, Gaussian, Wallingford, CA, USA (2009).

[63] R.G. Parr, W. Yang, Density Functional Theory of Atoms and Molecules Oxford University Press, Oxford (1989).

[64] R. Krishnan, J.S. Binkley, R. Seeger, J.A. Pople, Self-consistent molecular orbital methods. XX. A basis set for correlated wave functions, J. Chem. Phys. 72 (1980) 650. DOI: 10.1063/1.438955

[65] S. Hassen, M.O. Zouaghi, I. Slimani, Y. Arfaoui, N. Ozdemir, I. Ozdemir, N. Gurbuz, L. Mansour, N. Hamdi, J. Mol. Struct. 1265 (2022) 133397. DOI: 10.1016/j.molstruc.2022.133397

[66] M.A. Spackman, P.G. Byrom, Chem. Phys. Lett. 267 (1997) 215–220. DOI: 10.1016/S0009-2614(97)00100-0

[67] J.-J. Liu, S.-D. Jiang, P. Neugebauer, J. van Slageren, Y. Lan, W. Wernsdorfer, B.-W. Wang, S. Gao, Magnetic and HFEPR Studies of Exchange Coupling in a Series of μ-Cl Dicobalt Complexes, Inorg. Chem. 56 (2017) 2417–2425. DOI: 10.1021/acs.inorgchem.6b02368

[68] X-l. Wang, F.-f. Sui, H.-y. Lin, J-w. Zhang, G-c. Liu, Multifunctional Cobalt(II) Coordination Polymers Tuned by Flexible Bis(pyridylamide) Ligands with Different Spacers and Polycarboxylates, Cryst. Growth Des. 14 (2014) 3438–3452. DOI: 10.1021/cg500371n

[69] G. Resnati, E. Boldyreva, P. Bombiczd, M. Kawano, Supramolecular interactions in the solid state, IUCrJ. 2 (2015) 675-690. DOI: 10.1107/S2052252515014608

[70] M. Mirzaei, H. Eshghi, F.A. Bagherjeri, M. Mirzaei, A. Farhadipou, Investigation of non-covalent and hydrogen bonding interactions on the formation of crystalline networks and supramolecular synthons of a series of α-aminophosphonates: Crystallography and DFT studies, J. Mol. Struct. 1163 (2018) 316-326. DOI: 10.1016/j.molstruc.2018.03.014

[71] D. Chen, N. Oezguen, P. Urvil, C. Ferguson, S.M. Dann, T.C. Savidge, Regulation of protein-ligand binding affinity by hydrogen bond pairing, Sci. Adv. 2 (2016) 2703. DOI: 10.1126/sciadv.1501240

[72] T- Steiner, The Hydrogen Bond in the Solid State, Angew. Chem., Int. Ed. 41 (2002) 48–76. DOI: 1433-7851/02/4101-0049 $ 17.50+.50/0

[73] S. Hassen, Y. Arfaoui, K. Robeyns, T. Steenhaut, Y. Filinchuk, A. Klein, H. Chebbi, Architecture of a dinuclear Co(II) complex based on 3-amino-1,2,4-triazole-5-carboxylic acid: molecular structure, thermal behavior, optical properties, and DFT calculations, J. Coord. Chem. 75 (2022) 908–924. DOI: 10.1080/00958972.2022.2090246

[74] J.Y. Gao, N. Wang, X.H. Xiong, C.J. Chen, W.P. Xie, X.R. Ran, Y. Long, S.T. Yue, Y.L. Liu, Syntheses, structures, and photoluminescent properties of a series of zinc(II)–3-amino-1,2,4-triazolate coordination polymers constructed by varying carboxylate anions, CrystEngComm. 15 (2013) 3261. DOI: 10.1039/C3CE00049D

[75] S. Hassen, H. Chebbi, Y. Arfaoui, M.F. Zid, Synthesis of $[MnCl_3(H_2O)_2(Hatz)]\cdot H_2O$ and investigation of its structure via X-ray diffraction, spectroscopic measurements and DFT calculations, J. Iran. Chem. Soc. 15 (2018) 2659–2668, DOI: 10.1007/s13738-018-1454-4v

[76] M.B. Bushuev, A.V. Virovets, Y. Garcia, C. Gieck, L.A. Sheludyakova, V.N. Ikorskii, W. Tremel, P. Gütlich, L.G. Lavrenova, Mononuclear coordination compounds based on a novel chelating triazole ligand: 1-vinyl-3-acetylamino-1,2,4-triazole, Polyhedron 24 (2002) 797–804. DOI: 10.1016/S0277-5387(02)00844-6

[77] M. Yin, C. Wu, X. Yang, Y. Wang, Y. Fan, Synthesis, Crystal Structure, and Characterization of a New Zinc Complex with Flexible Ligand (4-Amino-1,2,4-triazole-3,5-diyldithio)diacetic Acid and 4,4′-Bipyridine, Synth. React. Inorg., Met.-Org., Nano-Met. Chem. 40 (2010) 798–804. DOI: 10.1080/15533174.2010.522546

[78] M.S. Refa, R.F. De Farias, Synthesis, characterization and thermogravimetric study of Cu(II) adducts with 3- and 4-amino-1,2,4-triazole, 2-mercaptothiazoline and 2-mercaptopyridine, J. Serb. Chem. Soc. 71 (2006) 1289–1300. DOI: 10.2298/JSC0612289R

[79] S.H. Sumrra, W. Zafar, M.L. Asghar, F. Mushtaq, M.A. Raza, M.F. Nazar, M.A. Nadeem, M. Imran, S. Mumtaz, Computational investigation of molecular structures, spectroscopic properties, cholinesterase inhibition and antibacterial activities of triazole Schiff bases endowed metal chelates, J. Mol. Struct. 1238 (2021) 130382. DOI: 10.1016/j.molstruc.2021.130382

[80] I. Matulková, I. Němec, K. Teubner, P. Němec, Z. Mička, Novel compounds of 4-amino-1,2,4-triazole with dicarboxylic acids – crystal structures, vibrational spectra and non-linear optical properties, J. Mol. Struct. 873 (2008) 46–60. DOI: 10.1016/j.molstruc.2007.03.007

[81] P. Kamalakannan, D. Venkappayya, Synthesis and characterization of cobalt and nickel chelates of 5-dimethylaminomethyl-2-thiouracil and their evaluation as antimicrobial and anticancer agents, J. Inorg. Biochem. 90 (2002) 22–37. DOI: 10.1016/S0162-0134(02)00413-0

[82] L. Mărutescu, L. Calu, M.C. Chifiriuc, C. Bleotu, C.-G. Daniliuc, D. Fălcescu, C.M. Kamerzan, M. Badea, R. Olar, Synthesis, Physico-chemical Characterization, Crystal Structure and Influence on Microbial and Tumor Cells of Some Co(II) Complexes with 5,7-Dimethyl-1,2,4-triazolo[1,5-a]pyrimidine, Molecules 22 (2017) 1233. DOI: 10.3390/molecules22071233

[83] A.O. Kshetry, N.D. Pant, R. Bhandari, S. Khatri, K.L. Shrestha, S.K. Upadhaya, A. Poudel, B. Lekhak, B.R. Raghubanshi, Minimum inhibitory concentration of vancomycin to methicillin resistant *Staphylococcus aureus* isolated from different clinical samples at a tertiary care hospital in Nepal, Antimicrob. Res. Infect. Control 5 (2016) 27 (1–6). DOI 10.1186/s13756-016-0126-3

[84] L. Zhang, W. Yang, Y. Chu, B. Wen, Y. Cheng, T. Mahmood, M. Bao, F. Ge, L. Li, J. Yi, C. Du, C. Lu, Y. Tan, The Inhibition Effect of Linezolid with Reyanning Mixture on MRSA and its Biofilm is more Significant than that of Linezolid Alone, Front. Pharmacol. 12 (2022) 766309 (1–18). DOI: 10.3389/fphar.2021.766309

Declaration of interests

The authors declare that they have no known competing financial interests or personal relationships that could have appeared to influence the work reported in this paper.

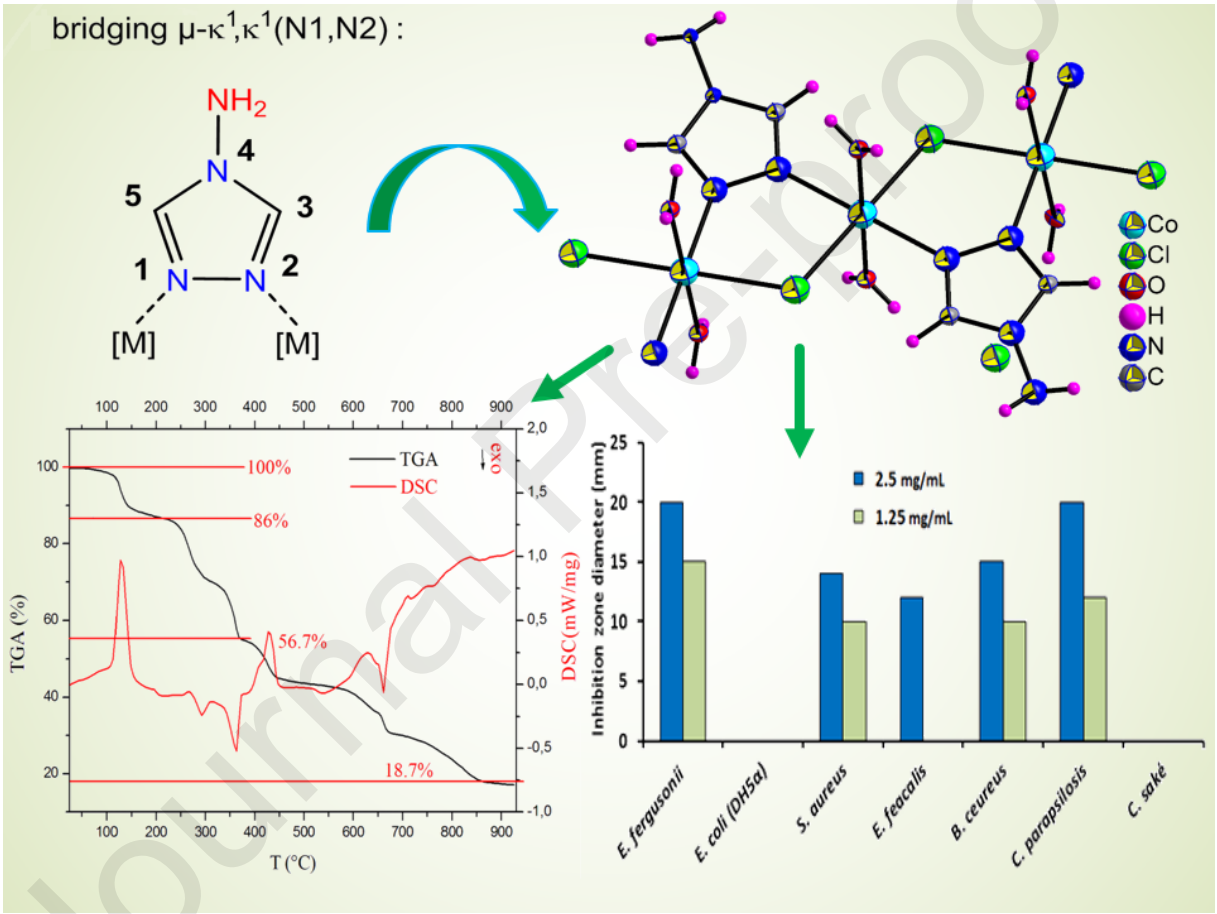
Highlights

- Co(II) coordination polymer $^{1}_{\infty}$[Co(μ-L)(μ-Cl)(H_2O)$_2$]Cl based on 4-amino-4*H*-1,2,4-triazole (L).
- Crystal structure with intra and intermolecular N–H···O and O–H···Cl hydrogen bonding interactions
- DFT geometry optimization for the model [Co(L)$_2$Cl$_2$(H_2O)$_2$] agrees well with the metrics found in the crystal structure.

- TGA and DSC experiments showed thermal stability till about 100°C.

- Inhibitory activity against the Gram-neg. bacterium *E. fergusonii*, the Gram-pos. bacteria *S aureus*, *E. feacalis*, and *B ceureus*, and the yeast *C. parapsilosis* was found.

- For the Gram-neg. *E. coli* and the yeast *C. saké* no inhibitory activity was found.



Journal Pre-proofs